Cerebral Cortex, December 2017;27: 5496–5508

doi: 10.1093/cercor/bhw317
Advance Access Publication Date: 13 October 2016
Original Article

ORIGINAL ARTICLE

Intrinsic Brain Hub Connectivity Underlies Individual Differences in Spatial Working Memory

Jin Liu, Mingrui Xia, Zhengjia Dai, Xiaoying Wang, Xuhong Liao, Yanchao Bi, and Yong He

State Key Laboratory of Cognitive Neuroscience and Learning & IDG/McGovern Institute for Brain Research, Beijing Normal University, Beijing 100875, China

Address correspondence to Mingrui Xia, State Key Laboratory of Cognitive Neuroscience and Learning & IDG/McGovern Institute for Brain Research, Beijing Normal University, Beijing 100875, China. E-mail: mxia@bnu.edu.cn

Abstract

Spatial working memory (SWM) is an important component of working memory and plays an essential role in driving high-level cognitive abilities. Recent studies have demonstrated that individual SWM is associated with global brain communication. However, whether specific network nodal connectivity, such as brain hub connectivity, is involved in individual SWM performances remains largely unknown. Here, we collected resting-state fMRI (R-fMRI) data from a large group of 130 young healthy participants and evaluated their SWM performances. A voxel-wise whole-brain network analysis approach was employed to study the relationship between the nodal functional connectivity strength (FCS) and the SWM behavioral scores and to further estimate the participation of brain hubs in individual SWM. We showed significant associations between nodal FCS and SWM performance primarily in the default mode, visual, dorsal attention, and fronto-parietal systems. Moreover, over 41% of these nodal regions were identified as brain network hubs, and these hubs' FCS values contributed to 57% of the variance of the individual SWM performances that all SWM-related regions could explain. Collectively, our findings highlight the cognitive significance of the brain network hubs in SWM, which furthers our understanding of how intrinsic brain network architectures underlie individual differences in SWM processing.

Key words: connectomics, default mode, functional connectivity, graph-theory, module

Introduction

As an important component of working memory, spatial working memory (SWM) is involved in the temporary maintenance, updating and integration of visuospatial information and is indispensable for the accurate localization and tracking of external stimuli during the performance of cognitive tasks (Baddeley and Hitch 1974; Baddeley 2002). A wide spectrum of individual differences in the SWM capacity has been well documented (Cornoldi and Vecchi 2003), and individual variability in SWM ability is closely related to general cognitive aptitudes, such as intelligence (Fry and Hale 1996). With the development of non-invasive neuroimaging technologies over the last 20 years, the brain mechanisms associated with SWM have gained increasing attention. Task-based functional neuroimaging studies consistently indicate that regional activations (e.g., lateral prefrontal and parietal cortices) and deactivations (e.g., medial prefrontal and parietal cortices) are associated with the SWM capacity (Courtney et al. 1998; D'Esposito et al. 1998; Schweinsburg et al. 2005; Curtis 2006; Vuontela et al. 2009), suggesting that widely distributed brain regions underlie individual SWM processing.

In the past two decades, advancements in resting-state functional magnetic resonance imaging (R-fMRI) (Biswal et al. 1995) have offered unique opportunities to explore non-invasively the spontaneous functional activities or the intrinsic functional architectures underlying human cognitive behaviors in the absence of goal-directed tasks. Spontaneous functional activities that occur during the resting-state have been proven to reflect underlying neuronal activities (Shmuel and Leopold 2008;

Wang et al. 2012). Specifically, the synchronization of spontaneous functional activities among brain regions, which is also termed intrinsic functional connectivity, underlies variabilities in cognitive performance, such as conceptual processing (Wei et al. 2012), face processing (Zhu et al. 2011), and N-back working memory (Hampson et al. 2006). Recently, functional connectomic analysis using R-fMRI and graph-theory provides a more comprehensive perspective for quantitatively describing the topological configuration of intrinsic functional brain networks (Bullmore and Sporns 2009; He and Evans 2010; Bullmore and Bassett 2011). Using these novel approaches, several studies have suggested that SWM capacity is supported by the global topology of the brain network (Stevens et al. 2012; Alavash et al. 2015; Magnuson et al. 2015). For example, individual SWM performance is facilitated by the high global efficiency and modularity of the whole-brain network (Stevens et al. 2012; Alavash et al. 2015). Magnuson et al. (2015) found that individual SWM performance was related to the mean strength of the functional connectivity within a specific functional system that involved the lateral prefrontal and parietal cortices. These studies highlighted that individual SWM processing requires global communication and functional integration in the brain networks.

It is worthy noting that connectomic studies have demonstrated that human brain networks include a set of highly connected regions called brain hubs, which are primarily involved in the medial and lateral prefrontal and parietal regions (Buckner et al. 2009; Tomasi and Volkow 2010; Zuo et al. 2012; Liao et al. 2013). These brain hubs play critical roles in global communication and are characterized by high rates of cerebral blood flow and glucose metabolism (Liang et al. 2013; Tomasi et al. 2013; van den Heuvel and Sporns 2013). Spatially, these hub regions largely overlap with regions that show regional activation/deactivation in SWM-related processing, as mentioned above. This, raises the possibility that brain hubs might significantly contribute to the high communication requirements of individual SWM processing. However, it remains largely unknown whether and how the intrinsic network connectivity in specific brain regions, especially the brain hubs, underlies individual variability in SWM performance.

To address this issue, we collected R-fMRI data and visuospatial working memory task performances from a large group of 130 young healthy participants. Using a voxel-wise whole-brain connectivity analysis approach, we comprehensively explored the potential contribution of the network nodal connectivity capacity to individual variability in SWM. Such a voxel-wise approach avoids parcellation-dependent influences on the topological architecture of brain networks (Smith et al. 2011; de Reus and van den Heuvel 2013). Given that the medial and lateral prefrontal and parietal cortices exhibit distributed regional activations and deactivations during SWM tasks (Curtis 2006; Vuontela et al. 2009) and primarily belong to network hubs during rest (Buckner et al. 2009; Liang et al. 2013; van den Heuvel and Sporns 2013), we hypothesized that 1) intrinsic functional connectivity patterns in these regions would be significantly related to the SWM processing capacity of participants and 2) functional network hubs would play an important role in individual variations in SWM performance.

Materials and Methods

Participants

In this study, we used a dataset that included 146 healthy college students from the Connectivity-based Brain Imaging Research Database (C-BIRD) collected at the Beijing Normal University. All of the participants were right-handed and had no history of neurological or psychiatric disorders. Written informed consent was obtained from each participant, and this study was approved by the Institutional Review Board of the State Key Laboratory of Cognitive Neuroscience and Learning at the Beijing Normal University. The data from 16 subjects were excluded for the following reasons: 1) 1 was a non-native Chinese language speaker; 2) 11 did not complete the SWM task; 3) 3 had significant head motion (above 2 mm or 2° in any direction, see "Image preprocessing") and 4) 1 was an extreme outlier based on the SWM task scores (above 3 standard deviations, SDs). The data from the remaining 130 participants (67 females; age: 22.8 ± 2.3 years old, range: 19–31 years old; education: 16.1 ± 1.8 years, range: 11–23 years) were used for further analyses.

Image Acquisition

Data acquisition was performed using a Siemens Trio Tim 3.0 T scanner (Siemens Medical Systems, Erlangen, Germany) with a 12-channel phased-array head coil in the Imaging Center for Brain Research at the Beijing Normal University. The participants were instructed to rest and relax with their eyes closed and to refrain from falling asleep during the scan. The R-fMRI data were obtained using an echo-planar imaging sequence with following parameters: repetition time (TR)/echo time (TE) = 2000 ms/30 ms; flip angle (FA) = 90°; field of view (FOV) = 200 × 200 mm^2; matrix = 64 × 64; slices = 33; thickness = 3.5 mm; voxel size = 3.1 × 3.1 × 3.5 mm^3; gap = 0.7 mm and 200 volumes. The T1-weighted data were acquired using sagittal 3D magnetization prepared rapid gradient echo sequences. The sequence parameters were as follows: TR/TE = 2530 ms/3.39 ms; FA = 7°; FOV = 256 × 256 mm^2; matrix = 256 × 192; number of slices = 144; thickness = 1.3 mm and voxel size = 1 × 1.3 × 1.3 mm^3.

Behavioral Tests

Each participant performed an SWM task and a verbal working memory (VWM) task (Fig. 1) (Jonides et al. 1993; Smith et al. 1996). The SWM task was used to assess the visuospatial working memory processing ability of each participant. The VWM task was used as a control task to assess VWM processing ability, which provides an opportunity to reveal the relative

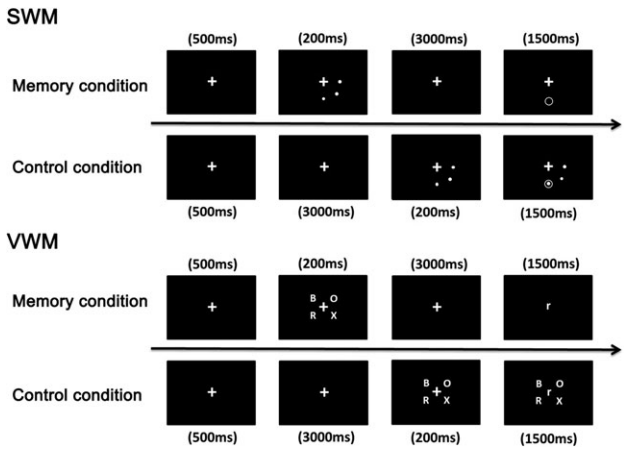

Figure 1. The flow charts of SWM and VWM tasks. The experimental procedures can be found in the methods section.

specificity of the findings for SWM. Visual stimuli were presented, and the responses were collected using E-Prime (Psychology Software Tools) in both tasks. These SWM and VWM tasks were conducted after the R-fMRI scans, and the participants were not told about the collection of behavioral data until the imaging scans were finished. Given that previous studies have suggested that prior experiences of task performance significantly affect subsequent R-fMRI data collection (Tung et al. 2013; Sami et al. 2014), our procedure ensured that the participants could not specifically think of the behavioral tasks during the scan to avoid data contamination. Several other behavioral tasks were also administered for specific research purposes and were not analyzed here.

SWM Task

We adopted the SWM task paradigm designed by Jonides et al. (1993). Briefly, the SWM task included 80 trials. Considering the potential individual variations in peripheral motor and perceptual processing, two conditions (a memory condition and a control condition) were included in this task. In the memory condition, in each trial, 3 dots were presented for 200 ms at various locations on a screen. After the 3 dots disappeared, a probe circle was presented for 1500 ms, during which the participants were required to press the corresponding buttons to judge whether the probe marked the location of any of the previous dots. The procedure of the control condition was the same as the memory condition except that the 3 dots and the probe circle appeared simultaneously, and after which, the participants were asked to judge whether the probe encircled a dot or not. Before the formal behavioral experiments, each participant performed 20 practice trials.

VWM Task

The VWM task (Smith et al. 1996) was very similar to the SWM task in the experimental structure, including the memory and control conditions. Briefly, four uppercase letters appeared on the screen simultaneously for 200 ms during the memory condition. After the letters disappeared, a lowercase letter was shown as a probe for 1500 ms, and the participants responded by pressing a button to indicate whether the probe had the same name as any of the letters that were shown prior to it.

Notably, different experimental materials (dots or letters) in these two tasks were used to assess different working memory processing. In this study paradigm, the SWM task, with the dots as the experimental stimuli, focuses on the spatial position information processing; whereas, the VWM task, with letter stimuli, reflects verbal information processing.

Data Analysis

Behavioral Data Analysis

To correct for any individual speed-accuracy trade-off effects, we calculated the inverse efficiency (IE) score (Townsend and Ashby 1983) as a behavioral measure of both the memory and control conditions in each task. The IE score was calculated by dividing the average response time of the correct trials by the accuracy across all trials. Subsequently, we reversed the sign of the scores so that higher IE scores represented more efficient performances.

To assess the SWM performance for each participant, we calculated an SWM score for each participant by regressing the contribution of the IE score of the control condition from the IE score of the memory condition using a regression analysis. This procedure excluded potential individual variations in peripheral primary motor and perceptual processing. Subsequently, the SWM scores for each participant were converted to a z-score for normalization. Specifically, we scaled each participant's score by subtracting the average score across the participants and then dividing it by the SD of the SWM scores. Similarly, for each participant, we computed the normalized VWM score using the same procedure as the SWM score computation.

Image Preprocessing

All of the preprocessing was performed using the Statistical Parametric Mapping software (SPM8; www.fil.ion.ucl.ac.uk/spm) and the Data Processing Assistant for Resting-State fMRI (DPARSF) (Chao-Gan and Yu-Feng 2010). Briefly, the first 5 volumes of the functional images were discarded for magnetic field stabilization and the participants' adaptation to the scanning environment. The subsequent preprocessing steps included slice time correction and head motion correction. Three subjects were excluded from the subsequent analyses due to significant head motion (above 2 mm or 2° in any directions). Next, the corrected functional images were normalized to the Montreal Neurological Institute (MNI) space by using a T1 image unified segmentation and were resampled to 3 mm isotropic voxels, followed by spatial smoothing with a 4 mm full-width at half-maximum Gaussian kernel. After the linear trends were removed, a temporal band-pass filter (0.01–0.1 Hz) was applied to reduce the low-frequency drift and high-frequency physiological noise. Finally, 6 head motion parameters and 3 other confounding signals (white matter, cerebrospinal fluid and global signals) were regressed from the time course of each voxel. The resultant residuals were used for the functional connectivity analyses.

Voxel-Wise Network Nodal Connectivity Measurements

To assess network connectivity, for each participant, we first computed the Pearson's correlations between the time series of all pairs of voxels within a gray matter mask with 45 892 voxels (gray matter probability values higher than 0.2 in the SPM gray matter template) to yield a whole-brain functional connectivity matrix. To improve the normality of the correlations, we transformed the individual correlation matrices to z-score matrices by using a Fisher's r-to-z transformation. Then, a threshold (here, $r = 0.2$, the threshold effects were evaluated in the "Validation Analysis") was chosen to eliminate the weak correlations attributable to signal noise. Finally, for each voxel, we calculated its functional connectivity strength (FCS) as the sum of the weight (z-values) of the connections between a given voxel and all of the other voxels. Notably, the FCS metric, which is referred to as the "degree centrality" of the weighted networks in terms of graph-theory, captures the global communication ability of brain regions in the whole networks (Buckner et al. 2009; Zuo et al. 2012; Liao et al. 2013) and reflects the rate of cerebral blood flow and metabolic levels (Liang et al. 2013; Tomasi et al. 2013). Considering the ambiguous interpretation of negative correlations with the removal of the global signal (Murphy et al. 2009), we conservatively restricted our analysis to positive correlations.

Correlation Between Behavior and Network Nodal Connectivity

To determine whether network nodal connectivity is significantly related to individual SWM performances, we performed a voxel-wise correlation analysis between the participants' SWM scores and FCS values. A Monte Carlo simulation was

employed to correct for multiple comparisons using the AFNI software package (Version AFNI_2011_12_21_1014, compiled on 12 August 2015) (Cox 1996). The statistical significance level was set to $P < 0.05$ with a cluster size > 208 voxels (5616 mm^3) corresponding to a corrected $P < 0.05$. Two additional statistical thresholds (2 initial voxel thresholds, namely $P < 0.01$ and $P < 0.001$) and a non-parametric permutation test were also used to validate the corrections for multiple comparisons (for details, see Validation Analysis). To further ascertain how these SWM-related regions are anatomically distributed in the brain systems, we calculated the percentage of the significant voxels located in the 8 functional systems, including the default mode, visual, dorsal attention, fronto-parietal, ventral attention, cingulo-opercular, salience, and sensorimotor systems. The parcellation of these functional systems was extracted from a prior brain template (Power et al. 2011). Moreover, to investigate with what regions these SWM-related regions were functionally connected, we considered a 5 mm sphere at each peak of the SWM-related cluster as a seed and performed a seed-based whole-brain functional connectivity analysis. Then, one-sample *t*-tests were used to determine significant functional connectivity with each peak across participants, and a Monte Carlo simulation was again employed to correct for multiple comparisons for each connectivity analysis.

Involvement of Brain Hubs in SWM

Previous studies have suggested that network hubs play important roles in global brain communication (Achard et al. 2006; Buckner et al. 2009; He et al. 2009). Considering that SWM processing involves global information integration in the whole brain (Alavash et al. 2015), we examined whether the regions showing significant correlations between FCS and SWM occupied central positions in the brain networks. Of the case, 2 strategies were used. 1) For each participant, we first computed the mean FCS within the SWM-related regions and the mean FCS of the other regions. Then, paired-sample *t*-tests were performed to determine whether the SWM regions had higher FCS values than all of the other regions in the brain. 2) To further explore the involvement of brain hubs in the individual SWM performances, we first obtained a group-level FCS map by averaging the individual FCS maps and then defined the brain network hubs by identifying voxels with higher FCS values (2 thresholds were used here: above 1 SD of the mean, which indicates a relatively stringent hub threshold, and above the mean, which indicates a relatively conservative hub threshold). For a given nodal voxel, higher FCS values indicate denser overall connections with other nodal voxels, which represent better functional communication or information integration over the brain (Buckner et al. 2009; Cao et al. 2014). Then, we computed the hub proportion, P_{hub}, namely, the proportion of SWM-related regions belonging to the brain hubs as

$$P_{hub} = \frac{N_{SWM \cdot hub}}{N_{SWM}} \times 100\%, \quad (1)$$

where $N_{SWM \cdot hub}$ is the number of common voxels between the SWM-related regions and the brain hubs, and N_{SWM} is the number of voxels within the SWM-related regions. Finally, non-parametric permutation tests were performed to examine whether this hub proportion was significantly higher than random. Briefly, an empirical distribution of the hub proportion was obtained by allocating random positions for the same number of voxels of the SWM-related regions and re-computing the P_{hub} of the randomized regions (10 000 permutations). The 95th percentile points of the empirical distribution were used as critical values in a one-tailed test of whether the observed hub proportion could occur by chance.

Within the SWM-related regions, we further investigated the contribution of brain hubs in explaining individual SWM performance. A 5-step procedure was undertaken as follows. First, we explored the total contributions of the SWM-related regions in explaining the variability of SWM performance. A linear regression analysis (model A) was performed, with the SWM score as the dependent variable and the averaged FCS value within all regions that showed significant SWM-FCS correlations as the independent variable. Second, we further explored the contributions of the overlapping hub regions (i.e., the voxels showing significant SWM-FCS correlations and simultaneously being identified as whole-brain hubs) in explaining the individual SWM performances. The linear regression analysis (model B) was performed with the SWM score as the dependent variable and the averaged FCS value within the overlapping hub areas as the independent variable. Third, we explored the contribution of the SWM-related regions and the overlapping hub regions in explaining the variability of SWM performance. A linear regression analysis (model C) was performed again, with the SWM score as the dependent variable and the averaged FCS values within all SWM-related regions and within the overlapping hub areas as the independent variables. Fourth, we compared the variance, R^2, of the model C with that of model A, resulting in a unique variance indicating that the overlapping hubs, but not the SWM-related regions, explained the variations in SWM. We further computed the shared variance (i.e., both the overlapping hub regions and all SWM-related regions could explain individual SWM performance) by subtracting the unique variance (model C vs. model A) from the variance that the hubs could explain (model B). Finally, the contribution ratio of hubs within the SWM-related regions was determined by dividing the total variance of all SWM regions (model A) by the shared variance.

Assessing the Relative Specificity of the Observed SWM Regions

To test whether the contribution of the network nodal connectivity of the obtained regions was relatively specific for SWM processing or general processing, we performed the following 2 analyses. First, we performed a voxel-wise correlation analysis between the VWM scores and the FCS values. The results were corrected for multiple comparisons, as described according to the previous procedure for SWM. Finally, we compared the results of the SWM and VWM analyses by counting the number of overlapping voxels between them. Second, we compared the SWM-FCS correlation coefficients to the VWM-FCS correlation coefficients by calculating a statistic z-value (Dunn and Clark 1969; Alavash et al. 2015) in a voxel-wise manner. Briefly, for a given voxel, the z-value was calculated as

$$z = \frac{\frac{1}{2}\ln\left(\frac{1+r_{SWM,FCS}}{1-r_{SWM,FCS}}\right) - \frac{1}{2}\ln\left(\frac{1+r_{VWM,FCS}}{1-r_{VWM,FCS}}\right)}{\sqrt{\frac{2(1-R)}{N-3}}}, \quad (2)$$

where N is the number of samples, $r_{SWM,FCS}$ is the SWM-FCS correlation coefficient, $r_{VWM,FCS}$ is the VWM-FCS correlation coefficient, and

$$R = \left(\frac{r_{SWM,VWM}(1 - r^2_{SWM,FCS} - r^2_{VWM,FCS}) - \frac{1}{2} r_{SWM,FCS} r_{VWM,FCS}(1 - r^2_{SWM,FCS} - r^2_{VWM,FCS} - r^2_{SWM,VWM})}{(1 - r^2_{SWM,FCS})(1 - r^2_{VWM,FCS})} \right), \quad (3)$$

where $r_{SWM,VWM}$ is the correlation coefficient between SWM and VWM scores.

In this study, we further evaluated the potential effects of differences in the measurement errors of SWM and VWM tasks while comparing the 2 correlations (Alavash et al. 2015). To do this, we first estimated the reliability of the SWM task using Cronbach's coefficient alpha (Cronbach 1951). Then, for each voxel, we obtained the corrected SWM-FCS correlation coefficient by dividing the original correlation coefficient by the square root of the reliability. The same procedure was also used to obtain the corrected VWM-FCS correlation coefficients. Finally, the statistic z-value was re-calculated to determine the significance of the differences between the SWM-FCS and VWM-FCS correlations using formula (2).

Validation Analysis

Data Analysis Strategies

To validate our major results, we examined the influence of the different image preprocessing and data analysis strategies. First, to assess the effects of demographic factors on our main results, we performed a general linear model analysis to examine the relationship between the FCS value and SWM score with age, gender, and years of education as covariates. Second, given that the spatial smoothing in the preprocessing steps might introduce artificial local correlations between voxels that were unrelated to their functional connections, we validated our major results without smoothing in our data preprocessing. Third, previous studies have suggested that global signals are associated with non-neuronal activity, such as respiration, and should therefore be removed (Fransson 2005; Birn et al. 2006; Fox et al. 2009). However, this processing introduces widespread negative functional connectivity and may alter the intrinsic correlation structure of brain networks (Murphy et al. 2009; Weissenbacher et al. 2009). Thus, we repeated our network analysis without global signal regression. Fourth, given that very local correlations may arise from aspects of data processing and head motion artifacts (Power et al. 2012), we excluded these very local correlations (<20 mm) during the FCS calculation procedure and re-performed the statistical analysis. Fifth, to determine whether our major results were dependent on the choices of correlation thresholds for connectivity, we recomputed the FCS maps using different correlation thresholds (i.e., 0.1, 0.3, 0.4, and 0.5) and then re-performed the statistical analysis. Finally, we further validated the effects of head motion on the estimation of functional connectivity by performing a "scrubbing" procedure (Power et al. 2012) on the preprocessed images. For the volumes with a frame-wise displacement exceeding a threshold of 0.5 mm, we replaced the volumes and their adjacent volumes (2 forward and 1 backward frames) with the nearest neighbor interpolated data within each subject's fMRI time series. We then re-identified the SWM-related regions using the scrubbed R-fMRI data.

Statistical Analysis Strategies

Several studies have suggested that different statistical analysis strategies could affect the fMRI results of multiple comparison corrections (Woo et al. 2014; Eklund et al. 2016). Thus, we evaluated the effects of different statistical analysis strategies on our main conclusions in 3 ways. First, we examined the effects of different initial voxel-level significance thresholds on our main results by using 2 other initial voxel-level thresholds (i.e., $P < 0.01$ and $P < 0.001$). Second, Eklund et al. (2016) suggested that the non-parametric permutation test could produce nominal results for both voxel-wise and cluster-wise inferences. Thus, we performed Spearman rank correlation to assess the relationship between SWM scores and FCS and further employed a non-parametric permutation test to determine the cluster-wise significance. Briefly, for each permutation, we first randomized individual SWM scores, re-performed the brain-behavior associations and recorded the maximal significant cluster size. With 10 000 permutations, an empirical distribution of the significant cluster size was obtained, and the 95th percentile points of the empirical distribution were used as critical values to determine whether the observed significant clusters occurred by chance. Finally, to validate the robustness of our main results, we performed a split-half reproducibility analysis by randomly dividing all participants into 2 independent subgroups matched for gender, age, years of education, and SWM scores (Table S1). Then, we repeated the voxel-wise SWM-FCS correlation analyses in each respective subgroup.

Table 1 Participants' performance on behavioral tasks

Task	Response time (ms) Mean ± SD (range)	Accuracy (%) Mean ± SD (range)	Inverse efficiency Mean ± SD (range)
SWM task (N = 130)			
Memory condition	761 ± 122 (443–1080)	82 ± 8 (0.60–0.98)	−942 ± 211 (−1728 to −522)
Control condition	583 ± 86 (411–902)	98 ± 2 (0.90–1)	−594 ± 92 (−945 to −411)
SWM score			0.87 ± 148 (−440 to 355)
VWM task (N = 129)[a]			
Memory condition	811 ± 103 (583–1058)	84 ± 10 (0.48–1)	−987 ± 198 (−1794 to −614)
Control condition	947 ± 109 (643–1207)	91 ± 6 (0.75–1)	−1050 ± 152 (−1470 to −713)
VWM score			−0.25 ± 190 (−1353 to 386)

[a]One participant was excluded as an extreme outlier on the VWM test scores (>3 SDs above the mean value). N, number of subject.

Results

SWM Correlated with the Network Nodal Connectivity

Table 1 shows the mean value and SD of the performance of all participants on the behavioral tasks, including the response times, accuracies, IE values and task scores. The distribution of the SWM scores followed a normal distribution (Kolmogorov–Smirnov test, $P = 0.20$) (Fig. 2A). The voxel-wise correlation analysis revealed significant positive correlations between the SWM scores and the FCS values, primarily in the bilateral posterior cingulate cortex/precuneus (PCC/PCU), the bilateral medial prefrontal cortex (MPFC), the left superior frontal gyrus (SFG), the bilateral inferior parietal lobules/intraparietal sulcus (IPL/IPS) and the medial occipital cortex (Fig. 2B,C and Table 2). These results indicate that higher nodal functional integration in regions corresponds to better individual SWM performance. Moreover, using a predefined functional modular template (Power et al. 2011), we showed that these SWM-related regions were predominantly distributed in the default mode (38%), visual (22%), dorsal attention (8%) and fronto-parietal (7%) systems (Fig. 2B). Finally, the seed-based whole-brain functional connectivity analyses (Fig. 3) provided further support for the findings in these brain systems.

Involvement of the Functional Network Hubs in SWM

To examine whether the regions showing significant SWM-FCS correlations occupied a central position in the global network integration, we compared the mean FCS between the SWM-related regions and the other regions and calculated the hub proportion of the SWM-related regions. First, we found that regions with significant SWM-FCS associations exhibited a higher FCS value than other regions ($t_{(df=129)} = 21.35$, $P = 3.70 \times 10^{-44}$) (Fig. 4A), suggesting that these SWM-related regions play more important roles in global brain communication. Second, we identified highly centralized hubs of the brain functional networks using a stringent FCS threshold (i.e., above 1 SD of the mean FCS) and found that they were predominantly located in the PCC/PCU, the MPFC, the lateral frontal and the parietal cortices (Fig. 4B). This spatial distribution of the brain hubs was largely compatible with previous findings (Buckner et al. 2009; Liang et al. 2013; Liao et al. 2013). Further analysis confirmed that, among the regions with significant SWM-FCS correlations, 41% (i.e., P_{hub}) belonged to the hub areas of the whole-brain networks (red color, Fig. 4C), and this proportion was significantly higher than that at a random level (permutation test, $P < 0.0001$). Notably, while using a conservative threshold (above the mean FCS) to define the brain hubs, we

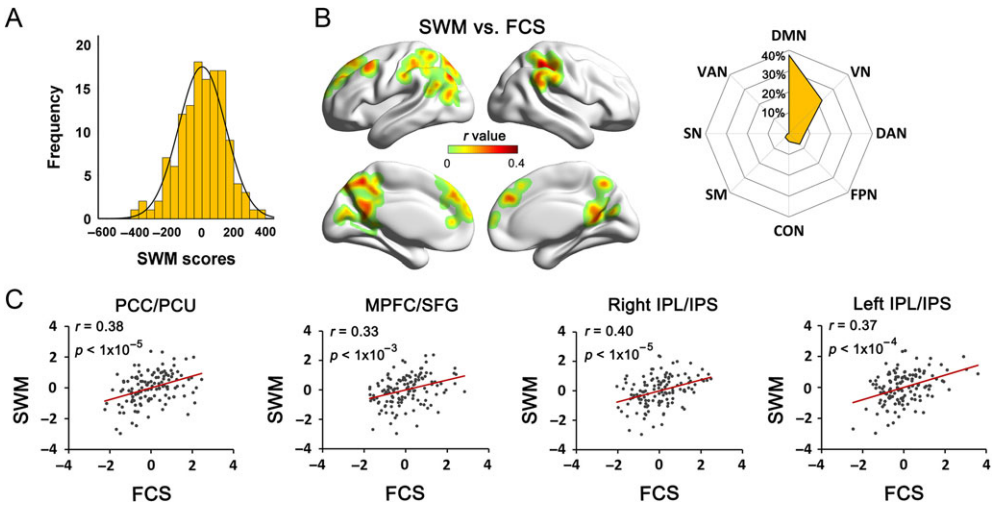

Figure 2. Distribution of individual SWM scores and the relationship between the nodal FCS and SWM scores. (A) The distribution of the SWM scores obeyed a normal distribution (Kolmogorov–Smirnov test, $P = 0.20$). (B) Left: Regions showing significant correlations between the FCS value and SWM performance. The significance threshold was set to the corrected $P < 0.05$ (single voxel $P < 0.05$, cluster size > 208 voxels). The r values were mapped on the cortical surface using BrainNet Viewer (Xia et al. 2013). Right: The system-dependent distribution of the significant regions. These significant regions are preferentially located in the default mode (38%), visual (22%), dorsal attention (8%) and fronto-parietal (7%) systems. (C) Scatter plots show positive correlations between the participants' SWM performances and the FCS of the cluster peak in the PCC/PCU, the MPFC/SFG, and the bilateral IPL/IPS. Here, the SWM and FCS values were converted to z-scores by subtracting the average value across the participants and dividing by the SD of the values. Each dot represents the data from one participant. DMN, default mode network; VN, visual network; DAN, dorsal attention network; FPN, fronto-parietal network; CON, cingulo-opercular network; SM, sensorimotor network; SN, salience network; VAN, ventral attention network.

Table 2 Regions showing significant correlation between FCS and SWM performance

Brain regions	BA	Peak MNI coordinates			T	Peak (r)			Voxels number
		x	y	z		IE	RT	ACC	
PCC/PCU	7,31	18	−51	15	4.65	0.38***	−0.27**	0.34***	1053
MPFC/SFG	8,9	3	42	36	4.01	0.33***	−0.10	0.16†	535
Right IPL/IPS	40,2	42	−45	54	4.90	0.40***	−0.17†	0.16†	426
Left IPL/IPS	40,2	−45	−39	54	4.57	0.37***	−0.24**	0.14	370

BA, Brodmann area; RT, response time; ACC, accuracy. *$P < 0.05$; **$P < 0.01$; ***$P < 0.001$; †$0.05 < P < 0.1$.

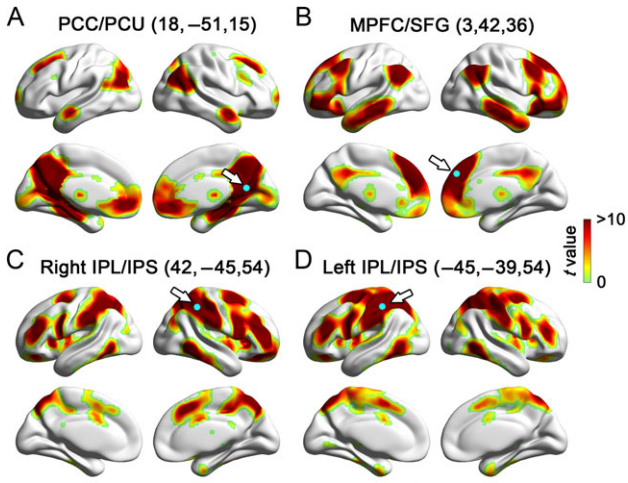

Figure 3. Seed-based functional connectivity maps of the SWM-related regions. The cyan dots in the brain maps indicate the seeds (i.e., the peaks of SWM-related regions) in the functional connectivity analysis. (*A*) The PCC/PCU (18 −51 15) and (*B*) the MPFC/SFG (3 42 36) exhibited significant functional connectivity mainly with the DMN; (*C*) the right IPL/IPS (42 −45 54) and (*D*) the left IPL/IPS (−45 −39 54) were functionally connected to the dorsal attention and the fronto-parietal networks. The significance level for these functional connectivity maps was set at $P < 0.001$ with cluster sizes > 51–59 voxels (varied for different maps), corresponding to a $P < 0.001$ corrected by Monte Carlo simulation.

found that 89% (i.e., P_{hub}) of the SWM-related regions were located at the hubs regions of the whole-brain networks, and this proportion was significantly higher than that at a random level (permutation test, $P < 0.0001$). Collectively, these results indicate that the regions with significant SWM-FCS correlations tend to have more crucial topological roles in global brain network integration.

Within the SWM-related regions, we further explored the contribution of brain hubs in explaining the individual SWM performance. When the averaged FCS value of SWM-related regions was entered into the regression as an independent variable, the model explained 21% of the variation in the participants' SWM processing efficiencies (model A: $R^2 = 0.21$; $F_{(1,128)} = 34.66$, $P = 3.25 \times 10^{-8}$) (Fig. 4*D*). When the averaged FCS value of the regions that overlapped the hubs (above 1 SD of the mean) was entered into the regression, the model explained 14% of the individual variation (model B: $R^2 = 0.14$; $F_{(1,128)} = 21.91$, $P = 7.19 \times 10^{-6}$) (Fig. 4*D*). When the averaged FCS value of the overlapping hubs (above 1 SD of the mean) and the averaged FCS value of all SWM-related regions were both entered in to the regression, the model explained 23% of the individual variation (model C: $R^2 = 0.23$; $F_{(2,127)} = 20.63$, $P = 1.74 \times 10^{-8}$). Thus, the unique variance that the overlapping hub regions could explain the variation of individual SWM performance was 0.02 (model C vs. model A: R^2: 0.23–0.21), while the shared variance of both the overlapping hub regions and all SWM-related regions was 0.12 (model B vs. (model C vs. model A): R^2: 0.14–0.02). Together, we found that the hub regions accounted for 57% (0.12/0.21) of the variation of the original interpretation model A (Table 3). Notably, while using the conservative threshold to define the hubs (above the mean), the model explained 20% of the individual variation ($R^2 = 0.20$; $F_{(1,128)} = 32.41$, $P = 8.11 \times 10^{-8}$), accounting for 81% of the original interpretation model (Table 3). Collectively, the FCS of the overlapping hub areas largely explained the variation that all of the SWM-related regions could explain in the variability of SWM processing, thus highlighting the important role of the hubs in SWM.

Functional Specificity of the Observed SWM-Related Regions

There was a low correlation between the behavioral scores of the SWM and VWM ($r = 0.18$, $P = 0.04$). Using a voxel-wise correlation analysis, we found that the FCS of the right hippocampus extending to the fusiform gyrus was negatively correlated with the VWM (Fig. S1A), which was largely different from the SWM-FCS correlation pattern. For the VWM-related regions (i.e., the right hippocampus and the fusiform gyrus), the seed-based functional connectivity pattern rarely overlapped with those of the SWM-related regions (Fig. S2). Notably, this result was also obtained by only using the IE score of the memory condition in the VWM task without considering the control condition (Fig. S1B).

Using the Dunn and Clark's statistic z-value, we compared the correlations between FCS and 2 working memory scores ($r_{SWM\text{-}FCS} - r_{VWM\text{-}FCS}$). Significantly stronger SWM-FCS correlations were found in the PCC/PCU, the MPFC/SFG and the IPL/IPS (Fig. S1C). This pattern was found even after controlling the reliabilities in the 2 tasks (Fig. S1D; The Cronbach's alpha of the SWM task was 0.67 and 0.72 for the VWM task). Together, these findings indicated the relative specificity of the contributions of the network nodal connectivity within most of these regions for SWM processing.

Reproducibility of the Main Results

We evaluated the reproducibility of our main findings under different image preprocessing procedures and data and statistical analysis strategies. The results remained consistent under these different strategies, as indicated by the high frequency of the spatial overlap of the SWM-related regions among validations, especially in the brain hubs such as the bilateral PCC/PCU, the bilateral MPFC, the left SFG, and the bilateral IPL/IPS (Fig. 5). See Fig. S3 for details of the validation results. Moreover, we performed a split-half analysis and found that the FCS in the medial and lateral parietal cortex was positively correlated with individual SWM performance in both subgroups (Fig. S4), suggesting the robust reproducibility of our main findings.

Discussion

In this study, we found that the FCS in the medial and lateral prefrontal and parietal regions was significantly correlated with individual SWM performances but was not correlated with the performance of the non-SWM task (i.e., VWM). These regions are predominantly located in the default mode, visual, dorsal attention and fronto-parietal systems. More importantly, these regions exhibited a high FCS and occupied a large hub proportion, they explaining 21% of the variation in the participants' SWM processing performances, of which the hub regions occupied 57% of this contribution. These findings indicated an intrinsic functional network organization underlying the individual differences in the SWM performances, and the brain hubs served as indispensable part of the organization.

Functional Systems Underlying Individual Differences in SWM Processing

Default Mode System

Notably, we found that most (38%) of the SWM-related regions were predominantly located in the default mode network (DMN), which has been demonstrated to exhibit deactivation during an SWM task (Vuontela et al. 2009). Anticevic et al. (2010)

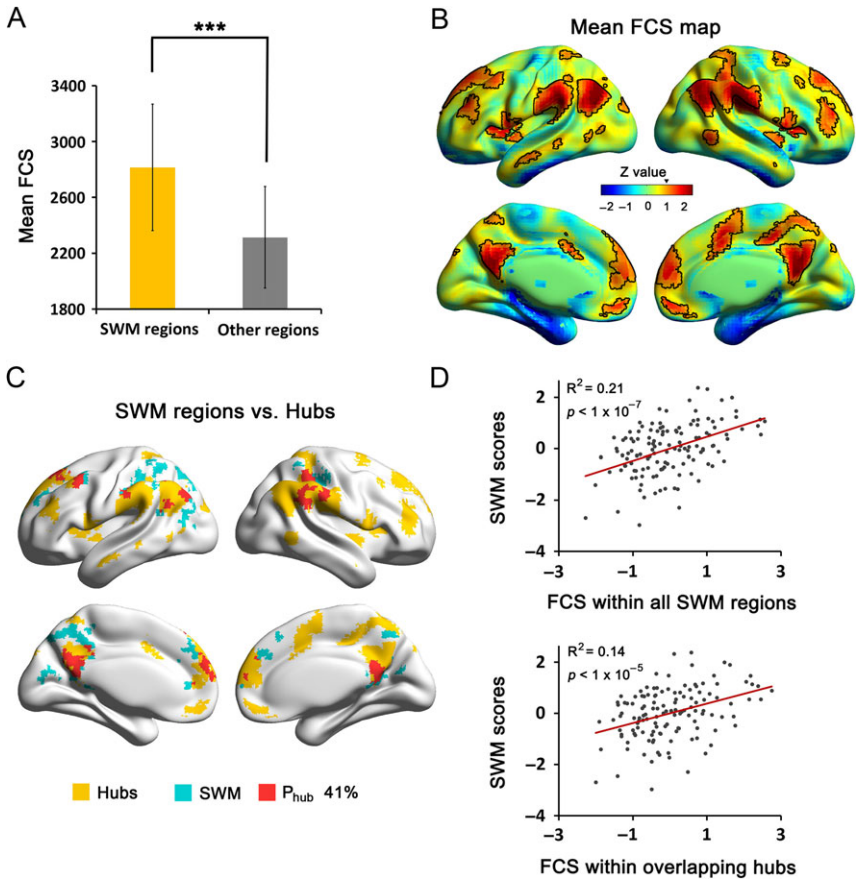

Figure 4. Functional hubs in the brain networks and their relationship with SWM. (*A*) The bar map shows that the mean FCS value within the regions showing significant FCS-SWM correlations was higher than the mean FCS value within other regions. The error bar represents the SD. ***P < 0.001. (*B*) The group-level mean FCS map was obtained by averaging the FCS maps across individuals. The hub areas (above 1 SD beyond the mean) are delineated with black lines. (*C*) The overlapping map between the regions contributing to individual differences in the SWM and the network hubs. The yellow patches indicate the hub areas, and the cyan patches indicate the SWM-related regions. The overlapping regions (41%, P_{hub}) are presented as red patches. (*D*) Scatter plots showing positive correlations between the participants' SWM performances and the mean FCS within all SWM-related regions (top) and the hubs overlapping with the SWM-related regions (bottom).

Table 3 Prediction of individual SWM performance by mean FCS

Regions	P_{hub}	*F*	df	R^2	*P*
All SWM-related regions		34.66	1,128	0.21	3.25×10^{-8}
All SWM-related regions + Overlapping hub regions (>1 SD + mean)		20.38	2,127	0.23	2.10×10^{-8}
Overlapping hub regions (>1 SD + mean)	41%	21.91	1,128	0.14	7.19×10^{-6}
All SWM-related regions + Overlapping hub regions (>mean)		20.63	2,127	0.23	1.74×10^{-8}
Overlapping hub regions (>mean)	89%	32.41	1,128	0.20	8.11×10^{-8}

P_{hub}, the proportion of SWM-related regions belonging to the brain hubs.

found that during a working memory task, deactivation in the DMN regions predicts individual working memory performance. Such deactivation likely means that the DMN reduces its activities during working memory tasks to ensure that limited attentional resources are directed towards task-relevant information and, thus, influences individual working memory processing. Moreover, the functional connectivity between the core DMN regions (e.g., PCC/PCU and MPFC) was correlated with individual working memory performance during tasks and at rest (Hampson et al. 2006; Esposito et al. 2009). In line with these previous studies, by analyzing the relationship between the individual differences in SWM performances and network nodal connectivity capability of the whole brain, our observations of the contribution of the FCS in the DMN to individual SWM performances further reinforce the notion that the function of the DMN not only involves internal mentation, such as self-referential processing, the theory of mind and future thinking (Buckner et al. 2008; Spreng et al. 2009), but also indirectly supports the performance of external-oriented processing, such as SWM (Liang et al. 2016).

Visual System

The visual system is one of the most important part involved visuospatial information integration in individual SWM processing. For instance, activation of the visual system was observed during perceptual processing in SWM (Courtney et al. 1997), and disrupted functional connectivity in the visual system has been observed in schizophrenia, associated with poor performance under a high-load SWM task conditions (Kang et al. 2011). Our results are in agreement with these previous findings showing that the resting FCS in the regions of the visual system are correlated with individual SWM performances.

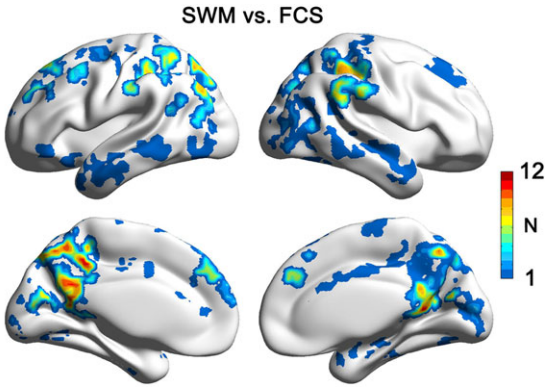

Figure 5. Conjunction map of the validation results. The brain map shows the frequencies of the spatial overlap of the SWM-related regions identified by nine different image preprocessing and data analysis strategies (including regressing out the demographic factors, performing smoothing during preprocessing, retaining the global signal, removing local connections, using four different connectivity thresholds and scrubbing for head motion), and three statistical analysis strategies (including two different initial voxel-level significance thresholds and a non-parametric permutation test). The regions with higher frequencies indicate higher stability in the validation analysis. *N*, the number of occurrences in the validations.

Moreover, previous studies have demonstrated that the fMRI signals of the visual cortex retain high fluctuations during the retention interval even when the visual stimulation disappeared during the SWM task (Munneke et al. 2010) and that the activity pattern in the visual cortex during the retention interval can successfully predict the orientation of the stimuli (Pratte and Tong 2014). Together with our findings, we suggest that the visual system not only participates in primary visual processing but is also involved in higher-level integrated processing, such as SWM.

Dorsal Attention and Fronto-Parietal Systems

The dorsal attention and fronto-parietal systems are traditionally considered as crucial components associated with SWM, as characterized by their consistent activation during various types of SWM tasks (Belger et al. 1998; Courtney et al. 1998; D'Esposito et al. 1998; Nystrom et al. 2000; Curtis 2006). Notably, brain regions in the dorsal attention and fronto-parietal systems may perform different processes in SWM processing. For example, information processing and motor planning involve the prefrontal cortex, while sensory information coding and storage are more prominent in the posterior parietal cortex (Curtis 2006; Eriksson et al. 2015). In line with this proposition, our experimental paradigm of SWM in this study mainly reflects spatial information coding and storage, and thus the functional connectivity in the posterior parietal cortex showed the most robust correlation with SWM (Fig. 5). Not only the local activations but also the functional connectivities representing interactions in the dorsal attention and fronto-parietal systems are involved in individual SWM performances. Recently, Bray et al. (2015) found that the functional connectivity within the fronto-parietal system during an SWM manipulation task increased according to the task demand. Magnuson et al. (2015) also found that the functional connectivity within the fronto-parietal system during the resting-state is associated with individual SWM performances. These studies, along with our findings, provide consistent evidence that the functional connectivity of the dorsal attention and fronto-parietal systems is crucial for individual SWM processing.

Involvement of the Hubs in the Variations in SWM Processing

The FCS, calculated by summing the connectivity strength of a given voxel with all the other voxels, might reflect the possible communicational resource of the region, capturing the global communication abilities of the whole networks (Buckner et al. 2009; Cole et al. 2012). Thus, brain regions with high FCS during the resting-state might imply their remarkable capacity for information transfer during the task state. These regions are identified as "hubs" in brain networks, which occupy a central position in the communication and integration of the brain network to support its diverse functional roles across a broad range of cognitive tasks (Cole et al. 2013; van den Heuvel and Sporns 2013). Our results showed that the SWM-related regions tended to have higher FCS values in the brain and had large areas of overlap with hub, and that the hubs explained most of the variation in explaining the SWM capacity. The involvement of a hub might facilitate two aspects of information communication and integration required by the SWM. First, the SWM requires the integration of massive amounts of information between the distributed regions across the brain in its intra-processes during task performance. Second, as the "workbench of cognition" (Klatzky 1975), the SWM requires heavy communication and integration with other high-level cognitive functions to support the performance of complex real-world activities involving a large amount of visuospatial information processing (Kyllonen and Christal 1990; Engle et al. 1999; Trick et al. 2012; Ashkenazi et al. 2013). Notably, the hubs occupied a central position in the communication and integration of the brain network, and thus, the involvement of hubs in SWM is optimal to satisfy the large integration requirement for SWM processing, supporting the information communication and integration required for both the intra-processes of SWM and cooperation with other high-level cognitive processes. A recent study showed that the densely connected regions reorganize the network architecture by increasing the regional flexibility and FCS to adapt the task demands during a working memory task (Vatansever et al. 2015). Such phenomena might suggest that the modulation of hub regions enhances the capability of processing a large quantity of information during a working memory task.

Interestingly, we observed different functional connectivity patterns between individual SWM and VWM processing, suggesting the relative functional specificity of network connectivity in two working memory tasks. These findings are supported by several previous studies. Specifically, an intriguing study by Alavash and colleagues (2015) showed that the VWM is primarily involved in verbal or number processing and is facilitated by local information integration. In contrast, SWM is primarily associated with the visuospatial processing, which requires the involvement of multiple regions and pathways to support the diversity of visuospatial functions (Kravitz et al. 2011). Moreover, Alavash et al. (2015) reported that visuospatial working memory was associated with high global network efficiency and modularity, suggesting that individual SWM processing requires global communication and functional integration of brain networks. It should be emphasized that we observed that SWM is involved in highly connected brain network hubs. Given that the network hubs play vital roles in global brain communication (Buckner et al. 2009; Liang et al. 2013), our findings provide further evidence of the global network integration architecture underlying individual SWM performance.

In this work, we showed the divergent mechanisms underlying SWM and VWM in the global integration of brain

networks. However, it is worthy to note that both the SWM and the VWM belong to working memory and could have common neural mechanisms to a certain degree. Based on previous studies (Kravitz et al. 2011; Alavash et al. 2015), we speculate that the common mechanisms between SWM and VWM could be involved in local brain activity. To explore this possibility, for each subject we calculated the amplitude of low-frequency fluctuations (ALFFs, a metric that reflects local brain activity) (Zang et al. 2007) in a voxel-wise manner and separately performed the ALFF-SWM and ALFF-VWM correlation analyses. We observed that both SWM and VWM showed significant correlations with ALFF in the superior parietal cortex (Fig. 6*A* and *B*). The region is usually considered as a critical region for general working memory processing and showed consistent activation during both SWM and VWM tasks (Wager and Smith 2003; Walter et al. 2003). Thus, these results suggest that, although the SWM and VWM exhibit divergent mechanisms in global integration at the network level, they share similar brain mechanisms at the local activity level. Future works should be conducted to systematically ascertain the convergence and divergence of the brain network substrates underlying individual SWM and VWM processing.

Methodological Considerations

Several methodological issues need to be further addressed. First, recent studies have demonstrated that several confounding factors might influence the results of functional connectivity analyses, particularly head motion (Power et al. 2012; Van Dijk et al. 2012) and removal of global signal (Scholvinck et al. 2010; Chai et al. 2012). Thus, we cautiously assessed these confounding effects and found that our main findings remained robust. Specifically, for head motion, we did not find a correlation between the averaged root mean square of head movement and SWM performance. However, we did not exclude the possibility that residual head motion signals might affect our results. Second, this study investigated the relationship between the intrinsic network connectivity strength in the functional brain network and the SWM scores. Recent studies have documented a close relationship between structural and functional networks (Honey et al. 2009; Wang et al. 2015). Thus, the structural foundation underlying the intrinsic functional network organization of individual SWM performances should be explored in a combined analysis of multimodal imaging data. Third, we focused our exploration on a group of young adults. Studying the SWM-related network in a cohort of children to adolescents is of great interest, which would allow us to delineate the developmental trajectory of the intrinsic functional connectivity organization underlying cognitive behaviors and to further expand the understanding of the formation of human cognitive functions. Finally, researches show that patients with mental illnesses, including schizophrenia, major depressive disorder and chronic alcoholism exhibit impaired performance in SWM tasks (Park and Holzman 1992; Sullivan et al. 1993; Murphy et al. 2003). The association between the intrinsic functional network organization and individual SWM performances is certainly worth exploring in disease states, which might provide potential predictive neuroimaging indicators for clinical applications and deepen our understanding the cognitive impairments in diseases.

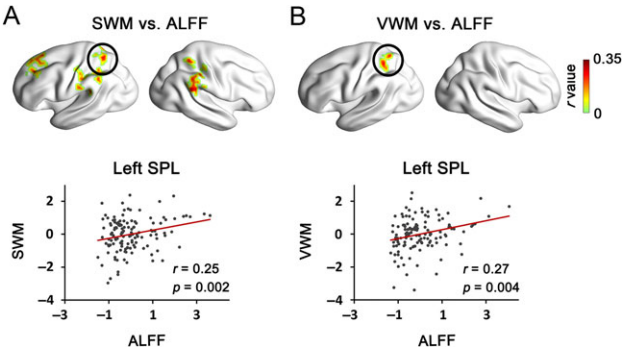

Figure 6. The relationship between the ALFF and SWM/VWM scores. (*A*) The brain map illustrates regions showing significant ALFF-SWM correlations. The scatter plot shows the positive correlation between the ALFF of the peak (−27 −54 63) of the left SPL and the participants' SWM performances. (*B*) The regions showing significant ALFF-VWM correlations. The scatter plot shows the positive correlation between the ALFF of the peak (−36 −54 60) of the left SPL and the participants' VWM performances. Of note, the SWM and ALFF values were converted to the z-scores by subtracting the average value across the participants and dividing by the SD of the values. Each dot represents the data from one participant. SPL, superior parietal lobule.

Conclusions

We demonstrated that the network nodal connectivity in the default mode, visual, dorsal attention, and fronto-parietal systems is highly associated with individual variations in SWM performance, and the brain hubs in these areas accounted for the majority of the contributions. These findings have multifaceted theoretical implications: 1) an intrinsic functional network organization underlies the individual differences in SWM, implying the importance of intrinsic network connectivity in the variance of SWM performances, and 2) brain hubs are involved in individual SWM performances, highlighting the significance of network hubs in cognitive function.

Supplementary Material

Supplementary material can be found at: http://www.cercor.oxfordjournals.org/

Funding

This study is financially sponsored through the 973 Program (Grant Nos. 2014CB846100 and 2013CB837300), the Fundamental Research Funds for the Central Universities (Grant No. 2015KJJCA13), the National Natural Science Foundation of China (Grant Nos. 91432115, 81401479, 81671767, and 81225012), and the Beijing Natural Science Foundation (Grant No. Z151100003915082 and Z16110100020000).

Notes

We thank Xindi Wang for help with data analyses and Qixiang Lin for help in data collection. *Conflict of Interest*: None declared.

References

Achard S, Salvador R, Whitcher B, Suckling J, Bullmore E. 2006. A resilient, low-frequency, small-world human brain functional network with highly connected association cortical hubs. J Neurosci. 26:63–72.

Alavash M, Doebler P, Holling H, Thiel CM, Giessing C. 2015. Is functional integration of resting state brain networks an

unspecific biomarker for working memory performance? Neuroimage. 108:182–193.
Anticevic A, Repovs G, Shulman GL, Barch DM. 2010. When less is more: TPJ and default network deactivation during encoding predicts working memory performance. Neuroimage. 49: 2638–2648.
Ashkenazi S, Rosenberg-Lee M, Metcalfe AWS, Swigart AG, Menon V. 2013. Visuo-spatial working memory is an important source of domain-general vulnerability in the development of arithmetic cognition. Neuropsychologia. 51:2305–2317.
Baddeley AD. 2002. Is working memory still working? Eur Psychol. 7:85–97.
Baddeley AD, Hitch G. 1974. Working memory. Psychol Learn Motiv. 8:47–89.
Belger A, Puce A, Krystal JH, Gore JC, Goldman-Rakic P, McCarthy G. 1998. Dissociation of mnemonic and perceptual processes during spatial and nonspatial working memory using fMRI. Hum Brain Mapp. 6:14–32.
Birn RM, Diamond JB, Smith MA, Bandettini PA. 2006. Separating respiratory-variation-related fluctuations from neuronal-activity-related fluctuations in fMRI. Neuroimage. 31:1536–1548.
Biswal B, Zerrin Yetkin F, Haughton VM, Hyde JS. 1995. Functional connectivity in the motor cortex of resting human brain using echo-planar mri. Magnet Reson Med. 34: 537–541.
Bray S, Almas R, Arnold AE, Iaria G, MacQueen G. 2015. Intraparietal sulcus activity and functional connectivity supporting spatial working memory manipulation. Cereb Cortex. 25:1252–1264.
Buckner RL, Andrews-Hanna JR, Schacter DL. 2008. The brain's default network: anatomy, function, and relevance to disease. Ann N Y Acad Sci. 1124:1–38.
Buckner RL, Sepulcre J, Talukdar T, Krienen FM, Liu H, Hedden T, Andrews-Hanna JR, Sperling RA, Johnson KA. 2009. Cortical hubs revealed by intrinsic functional connectivity: mapping, assessment of stability, and relation to Alzheimer's disease. J Neurosci. 29:1860–1873.
Bullmore E, Sporns O. 2009. Complex brain networks: graph theoretical analysis of structural and functional systems. Nat Rev Neurosci. 10:186–198.
Bullmore ET, Bassett DS. 2011. Brain graphs: graphical models of the human brain connectome. Annu Rev Clin Psychol. 7: 113–140.
Cao M, Wang JH, Dai ZJ, Cao XY, Jiang LL, Fan FM, Song XW, Xia MR, Shu N, Dong Q, et al. 2014. Topological organization of the human brain functional connectome across the lifespan. Dev Cogn Neurosci. 7:76–93.
Chai XJ, Castanon AN, Ongur D, Whitfield-Gabrieli S. 2012. Anticorrelations in resting state networks without global signal regression. Neuroimage. 59:1420–1428.
Chao-Gan Y, Yu-Feng Z. 2010. DPARSF: A MATLAB Toolbox for "Pipeline" data analysis of resting-state fMRI. Front Syst Neurosci. 4:13.
Cole MW, Yarkoni T, Repovs G, Anticevic A, Braver TS. 2012. Global connectivity of prefrontal cortex predicts cognitive control and intelligence. J Neurosci. 32:8988–8999.
Cole MW, Reynolds JR, Power JD, Repovs G, Anticevic A, Braver TS. 2013. Multi-task connectivity reveals flexible hubs for adaptive task control. Nat Neurosci. 16:1348–1355.
Cornoldi C, Vecchi T. 2003.Visuo-spatial working memory and individual differences. Hove: Psychology Press.
Courtney SM, Ungerleider BG, Keil K, Haxby JV. 1997. Transient and sustained activity in a distributed neural system for human working memory. Nature. 386:608–611.
Courtney SM, Petit L, Maisog JM, Ungerleider LG, Haxby JV. 1998. An area specialized for spatial working memory in human frontal cortex. Science. 279:1347–1351.
Cox RW. 1996. AFNI: software for analysis and visualization of functional magnetic resonance neuroimages. Comput Biomed Res. 29:162–173.
Cronbach LJ. 1951. Coefficient alpha and the internal structure of tests. Psychometrika. 16:297–334.
Curtis CE. 2006. Prefrontal and parietal contributions to spatial working memory. Neuroscience. 139:173–180.
D'Esposito M, Aguirre GK, Zarahn E, Ballard D, Shin RK, Lease J. 1998. Functional MRI studies of spatial and nonspatial working memory. Brain Res Cogn Brain Res. 7:1–13.
de Reus MA, van den Heuvel MP. 2013. The parcellation-based connectome: limitations and extensions. Neuroimage. 80: 397–404.
Dunn OJ, Clark V. 1969. Correlation coefficients measured on the same individuals. J Am Stat Assoc. 64:366–377.
Eklund A, Nichols TE, Knutsson H. 2016. Cluster failure: Why fMRI inferences for spatial extent have inflated false-positive rates. Proc Natl Acad Sci U S A. 113:7900–7905.
Engle RW, Tuholski SW, Laughlin JE, Conway AR. 1999. Working memory, short-term memory, and general fluid intelligence: a latent-variable approach. J Exp Psychol Gen. 128:309–331.
Eriksson J, Vogel EK, Lansner A, Bergstrom F, Nyberg L. 2015. Neurocognitive architecture of working memory. Neuron. 88:33–46.
Esposito F, Aragri A, Latorre V, Popolizio T, Scarabino T, Cirillo S, Marciano E, Tedeschi G, Di Salle F. 2009. Does the default-mode functional connectivity of the brain correlate with working-memory performances? Arch Ital Biol. 147:11–20.
Fox MD, Zhang D, Snyder AZ, Raichle ME. 2009. The global signal and observed anticorrelated resting state brain networks. J Neurophysiol. 101:3270–3283.
Fransson P. 2005. Spontaneous low-frequency BOLD signal fluctuations: an fMRI investigation of the resting-state default mode of brain function hypothesis. Hum Brain Mapp. 26: 15–29.
Fry AF, Hale S. 1996. Processing speed, working memory, and fluid intelligence: evidence for a developmental cascade. Psychol Sci. 7:237–241.
Hampson M, Driesen NR, Skudlarski P, Gore JC, Constable RT. 2006. Brain connectivity related to working memory performance. J Neurosci. 26:13338–13343.
He Y, Evans A. 2010. Graph theoretical modeling of brain connectivity. Curr Opin Neurol. 23:341–350.
He Y, Wang J, Wang L, Chen ZJ, Yan C, Yang H, Tang H, Zhu C, Gong Q, Zang Y, et al. 2009. Uncovering intrinsic modular organization of spontaneous brain activity in humans. PLoS One. 4:e5226.
Honey CJ, Sporns O, Cammoun L, Gigandet X, Thiran JP, Meuli R, Hagmann P. 2009. Predicting human resting-state functional connectivity from structural connectivity. Proc Natl Acad Sci U S A. 106:2035–2040.
Jonides J, Smith EE, Koeppe RA, Awh E, Minoshima S, Mintun MA. 1993. Spatial working-memory in humans as revealed by PET. Nature. 363:623–625.
Kang SS, Sponheim SR, Chafee MV, MacDonald AW. 2011. Disrupted functional connectivity for controlled visual

processing as a basis for impaired spatial working memory in schizophrenia. Neuropsychologia. 49:2836–2847.
Klatzky RL. 1975.Human memory: structures and processes. San Francisco: Freeman.
Kravitz DJ, Saleem KS, Baker CI, Mishkin M. 2011. A new neural framework for visuospatial processing. Nat Rev Neurosci. 12:217–230.
Kyllonen PC, Christal RE. 1990. Reasoning ability is (little more than) working-memory capacity?! Intelligence. 14:389–433.
Liang X, Zou Q, He Y, Yang Y. 2013. Coupling of functional connectivity and regional cerebral blood flow reveals a physiological basis for network hubs of the human brain. Proc Natl Acad Sci U S A. 110:1929–1934.
Liang X, Zou Q, He Y, Yang Y. 2016. Topologically reorganized connectivity architecture of default-mode, executive-control, and salience networks across working memory task loads. Cereb Cortex. 26:1501–1511.
Liao XH, Xia MR, Xu T, Dai ZJ, Cao XY, Niu HJ, Zuo XN, Zang YF, He Y. 2013. Functional brain hubs and their test-retest reliability: a multiband resting-state functional MRI study. Neuroimage. 83:969–982.
Magnuson ME, Thompson GJ, Schwarb H, Pan WJ, McKinley A, Schumacher EH, Keilholz SD. 2015. Errors on interrupter tasks presented during spatial and verbal working memory performance are linearly linked to large-scale functional network connectivity in high temporal resolution resting state fMRI. Brain Imaging Behav. 9:854–867.
Munneke J, Heslenfeld DJ, Theeuwes J. 2010. Spatial working memory effects in early visual cortex. Brain Cogn. 72: 368–377.
Murphy FC, Michael A, Robbins TW, Sahakian BJ. 2003. Neuropsychological impairment in patients with major depressive disorder: the effects of feedback on task performance. Psychol Med. 33:455–467.
Murphy K, Birn RM, Handwerker DA, Jones TB, Bandettini PA. 2009. The impact of global signal regression on resting state correlations: are anti-correlated networks introduced? Neuroimage. 44:893–905.
Nystrom LE, Braver TS, Sabb FW, Delgado MR, Noll DC, Cohen JD. 2000. Working memory for letters, shapes, and locations: fMRI evidence against stimulus-based regional organization in human prefrontal cortex. Neuroimage. 11:424–446.
Park S, Holzman PS. 1992. Schizophrenics show spatial working memory deficits. Arch Gen Psychiatry. 49:975–982.
Power JD, Barnes KA, Snyder AZ, Schlaggar BL, Petersen SE. 2012. Spurious but systematic correlations in functional connectivity MRI networks arise from subject motion. Neuroimage. 59:2142–2154.
Power JD, Cohen AL, Nelson SM, Wig GS, Barnes KA, Church JA, Vogel AC, Laumann TO, Miezin FM, Schlaggar BL, et al. 2011. Functional network organization of the human brain. Neuron. 72:665–678.
Pratte MS, Tong F. 2014. Spatial specificity of working memory representations in the early visual cortex. J Vis. 14:22.
Sami S, Robertson EM, Miall RC. 2014. The time course of task-specific memory consolidation effects in resting state networks. J Neurosci. 34:3982–3992.
Scholvinck ML, Maier A, Ye FQ, Duyn JH, Leopold DA. 2010. Neural basis of global resting-state fMRI activity. Proc Natl Acad Sci U S A. 107:10238–10243.
Schweinsburg AD, Nagel BJ, Tapert SF. 2005. fMRI reveals alteration of spatial working memory networks across adolescence. J Int Neuropsychol Soc. 11:631–644.
Shmuel A, Leopold DA. 2008. Neuronal correlates of spontaneous fluctuations in fMRI signals in monkey visual cortex: implications for functional connectivity at rest. Hum Brain Mapp. 29:751–761.
Smith EE, Jonides J, Koeppe RA. 1996. Dissociating verbal and spatial working memory using PET. Cereb Cortex. 6:11–20.
Smith SM, Miller KL, Salimi-Khorshidi G, Webster M, Beckmann CF, Nichols TE, Ramsey JD, Woolrich MW. 2011. Network modelling methods for FMRI. Neuroimage. 54:875–891.
Spreng RN, Mar RA, Kim AS. 2009. The common neural basis of autobiographical memory, prospection, navigation, theory of mind, and the default mode: a quantitative meta-analysis. J Cogn Neurosci. 21:489–510.
Stevens AA, Tappon SC, Garg A, Fair DA. 2012. Functional brain network modularity captures inter- and intra-individual variation in working memory capacity. PLoS One. 7:e30468.
Sullivan EV, Mathalon DH, Zipursky RB, Kersteen-Tucker Z, Knight RT, Pfefferbaum A. 1993. Factors of the Wisconsin Card Sorting Test as measures of frontal-lobe function in schizophrenia and in chronic alcoholism. Psychiatry Res. 46: 175–199.
Tomasi D, Volkow ND. 2010. Functional connectivity density mapping. Proc Natl Acad Sci U S A. 107:9885–9890.
Tomasi D, Wang GJ, Volkow ND. 2013. Energetic cost of brain functional connectivity. Proc Natl Acad Sci U S A. 110: 13642–13647.
Townsend JT, Ashby FG. 1983.Stochastic modeling of elementary psychological processes. Cambridge: Cambridge University Press.
Trick LM, Mutreja R, Hunt K. 2012. Spatial and visuospatial working memory tests predict performance in classic multiple-object tracking in young adults, but nonspatial measures of the executive do not. Atten Percept Psychophys. 74:300–311.
Tung KC, Uh J, Mao D, Xu F, Xiao GH, Lu HZ. 2013. Alterations in resting functional connectivity due to recent motor task. Neuroimage. 78:316–324.
van den Heuvel MP, Sporns O. 2013. Network hubs in the human brain. Trends Cogn Sci. 17:683–696.
Van Dijk KR, Sabuncu MR, Buckner RL. 2012. The influence of head motion on intrinsic functional connectivity MRI. Neuroimage. 59:431–438.
Vatansever D, Menon DK, Manktelow AE, Sahakian BJ, Stamatakis EA. 2015. Default mode dynamics for global functional integration. J Neurosci. 35:15254–15262.
Vuontela V, Steenari MR, Aronen ET, Korvenoja A, Aronen HJ, Carlson S. 2009. Brain activation and deactivation during location and color working memory tasks in 11–13-year-old children. Brain Cogn. 69:56–64.
Wager TD, Smith EE. 2003. Neuroimaging studies of working memory: a meta-analysis. Cogn Affect Behav Neurosci. 3: 255–274.
Walter H, Bretschneider V, Gron G, Zurowski B, Wunderlich AP, Tomczak R, Spitzer M. 2003. Evidence for quantitative domain dominance for verbal and spatial working memory in frontal and parietal cortex. Cortex. 39:897–911.
Wang L, Saalmann YB, Pinsk MA, Arcaro MJ, Kastner S. 2012. Electrophysiological low-frequency coherence and cross-frequency coupling contribute to BOLD connectivity. Neuron. 76:1010–1020.
Wang Z, Dai Z, Gong G, Zhou C, He Y. 2015. Understanding structural-functional relationships in the human brain: a large-scale network perspective. Neuroscientist. 21:290–305.

Wei T, Liang X, He Y, Zang Y, Han Z, Caramazza A, Bi Y. 2012. Predicting conceptual processing capacity from spontaneous neuronal activity of the left middle temporal gyrus. J Neurosci. 32:481–489.

Weissenbacher A, Kasess C, Gerstl F, Lanzenberger R, Moser E, Windischberger C. 2009. Correlations and anticorrelations in resting-state functional connectivity MRI: a quantitative comparison of preprocessing strategies. Neuroimage. 47: 1408–1416.

Woo CW, Krishnan A, Wager TD. 2014. Cluster-extent based thresholding in fMRI analyses: pitfalls and recommendations. Neuroimage. 91:412–419.

Xia M, Wang J, He Y. 2013. BrainNet Viewer: a network visualization tool for human brain connectomics. PLoS One. 8:e68910.

Zang YF, He Y, Zhu CZ, Cao QJ, Sui MQ, Liang M, Tian LX, Jiang TZ, Wang YF. 2007. Altered baseline brain activity in children with ADHD revealed by resting-state functional MRI. Brain Dev. 29:83–91.

Zhu Q, Zhang J, Luo YL, Dilks DD, Liu J. 2011. Resting-state neural activity across face-selective cortical regions is behaviorally relevant. J Neurosci. 31:10323–10330.

Zuo XN, Ehmke R, Mennes M, Imperati D, Castellanos FX, Sporns O, Milham MP. 2012. Network centrality in the human functional connectome. Cereb Cortex. 22:1862–1875.